*Preprints* (www.preprints.org) | NOT PEER-REVIEWED | Posted: 12 January 2017 doi:10.20944/preprints201701.0064.v1

# Identification of Secondary Phases in $Cu_2ZnSnS_4$ Layers by In-depth Resolved X-ray Photoelectron Spectroscopy Analysis

X. F. Zhang [1,*] and M. Kobayashi [2,3]

[1] International Center for Science and Engineering Programs, Waseda University, 3-4-1 Ookubou, Shinjyuku-ku, Tokyo 169-8555, Japan

[2] Department of Electrical Engineering and Bioscience, Waseda University, 3-4-1 Ookubou, Shinjyuku-ku, Tokyo 169-8555, Japan

[3] Kagami Memorial Research Institute for Materials Science, Waseda University, 3-4-1 Ookubou, Shinjyuku-ku, Tokyo 169-8555, Japan

Corresponding: zhangxf@aoni.waseda.jp

**Abstract**

A $Cu_2ZnSnS_4$ (CZTS) film with a thickness of approximately 1.5 μm was fabricated on a Mo-coated glass substrate by annealing a CZTS precursor fabricated from nanoparticle ink. The chemical states of the elements in the CZTS thin film in the depth direction were studied to identify the presence of secondary phases, which are detrimental to the performance of solar cells containing CZTS. X-ray diffraction was unable to detect any secondary phases in CZTS because of their small relative amount. Instead, X-ray photoelectron spectroscopy (XPS), which is highly sensitive to chemical state, was conducted at different depths in the CZTS film to further check the presence of secondary phases. XPS analysis revealed peaks shift consistent with the presence of secondary phases. For the CZTS film annealed in a S atmosphere at 575 °C for 3 h, the film surface consisted of a secondary-phase layer composed of CuS, ZnS, and $SnS_x$ ($x$=1 or 2) originating from the decomposition of CZTS. At depths below 80 nm, the film was pure CZTS. Formation of $MoS_2$ at the CZTS–Mo interface was confirmed by XPS analysis of Mo and S.

**Keywords**: secondary phases; CZTS film; XPS

---

## 1. Introduction

Kesterite $Cu_2ZnSnS_4$ (CZTS) has been recognized as a promising semiconductor for photovoltaic applications [1-3]. An efficiency of 12.6% has been achieved for a CZTS solar cell fabricated by a non-vacuum method [4]. The presence of secondary phases is a particularly serious problem for CZTS layers because they readily form due to the narrow region where

Preprints (www.preprints.org) | NOT PEER-REVIEWED | Posted: 12 January 2017 doi:10.20944/preprints201701.0064.v1

the pure kesterite phase exists [5, 6]. Fairbrother et al.[7] discussed the ability of secondary phases to degrade the performance of CZTS solar cells. However, secondary phases are difficult to detect by X-ray diffraction (XRD) because of their small relative amount [8]. X-ray photoelectron spectroscopy (XPS) is widely used to identify different atoms including very small amounts because of its high sensitivity to chemical state. However, application of XPS for the identification of secondary phases of CZTS films has not been reported up to know. In this work, XPS is conducted on a CZTS film after sputtering to identify the distribution of secondary phases in the depth direction.

## 2. Experimental Method

A CZTS film with a thickness of approximately 1.5 μm was fabricated on an Mo-coated glass substrate by annealing a CZTS precursor fabricated from CZTS nanoparticle ink under a S atmosphere in a glass tube. The CZTS ink and precursor were fabricated as we described elsewhere[9]. The annealing temperature was 575 °C, and annealing time was 3 h. After annealing, the CZTS film was exposed to air for less than 1 h before being set in the high-vacuum chamber (<$10^{-5}$ Pa) of an X-ray photoelectron spectrometer. Thus, the oxide layer on the surface of the film can be neglected. Energy-dispersive spectroscopy was performed on the CZTS film to determine its atomic ratios, which were identified as 0.93 for Cu/(Zn+Sn) and 0.32 for Zn/Sn.

## 3. Results and Discussions

Figure 1 shows the XRD pattern of the as-grown CZTS film before sputtering. Only peaks from kesterite CZTS were detected, indicating the pure CZTS phase was present [10]. To clarify the existence of secondary phases in the CZTS layer, XPS measurements were conducted using an Mg Kα X-ray source with a maximum photon energy of 1253.6 eV.

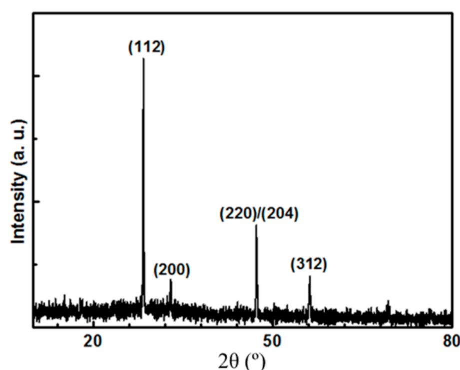


FIG. 1 XRD pattern of a typical as-grown CZTS film.

Preprints (www.preprints.org) | NOT PEER-REVIEWED | Posted: 12 January 2017 doi:10.20944/preprints201701.0064.v1

In-depth resolved XPS measurements were performed by sputtering the CZTS film with an $Ar^+$ beam generated by a magnetically controlled system attached to the XPS chamber. The power of the $Ar^+$ beam was controlled at 4.3 W with an acceleration voltage of 500 V and sputtering current of 8.6 μA to minimize the damage to the sputtered region. The sputtering rate was about 40 nm/min and sputtering times of 1, 2, 7, 15, and 35 min were used. After sputtering for each period, XPS measurements were conducted to determine the chemical state of atoms in the film.

Figure 2 shows the XPS data for oxygen at different depths in the CZTS film. Spectrum of oxygen atoms just showed up on the surface of the as-grown film. The broad oxygen peak between 530.2 and 534.5 eV on the surface of the CZTS film was attributed to surface attracted molecular oxygen, which has been discussed elsewhere [11]. After the film was sputtered of 40 nm (sputtering time: 1 min), the intensity of the oxygen peak decreased dramatically. When the film was sputtered further (sputtering time longer than 1 min), no oxygen peak was observed.

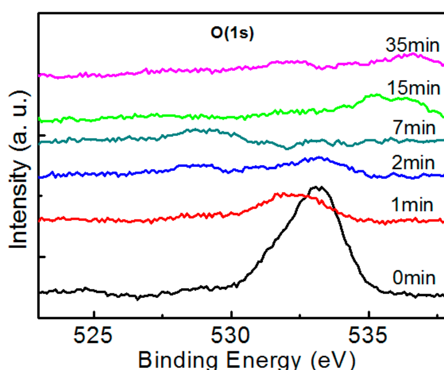


FIG. 2 XPS analysis of oxygen at different depths in the CZTS thin film. Before etching (sputtering time: 0 min), and after etching to depths of 40 nm (sputtering time: 1min), 80 nm (sputtering time: 2 min), 280 nm (sputtering time: 7 min), 600 nm (sputtering time: 15 min), and 1.4 μm (sputtering time: 35 min).

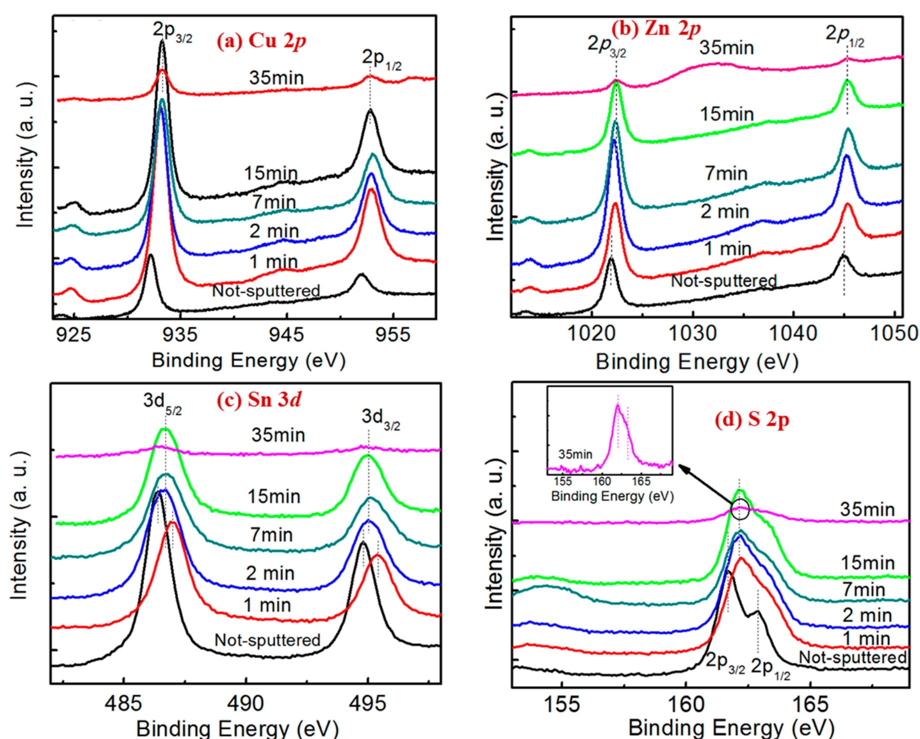


FIG. 3 XPS analysis at different depths in a CZTS layer. (a) Cu *2p*, (b) Zn 2*p*, (c) Sn 3*d*, and (d) S 2*p*. The inset is a magnified view of the S spectrum measured at the interface between CZTS and Mo.

Figure 3(a) shows the Cu 2*p* spectra obtained at different depths in the CZTS film. At the surface (before sputtering), two peaks were observed at binding energies of 932.3 and 952.3 eV, which shifted to 932.9 and 952.7 eV, respectively, after the film was sputtered for about 40 nm (sputtering time: 1 min). The position of the Cu 2*p* peaks did not change when the film was sputtered further, meaning that the chemical state of Cu did not change throughout the film depth. The intensity of the Cu 2*p* spectra increased dramatically after sputtering until the sputtering time was 35 min, at which time only weak peaks of Cu 2*p* were observed. This indicates that the whole CZTS film had been removed by sputtering and that the Mo layer was not yet sputtered. The peak around 932 eV was assigned to Cu $2p_{3/2}$, while that at around 952 eV was attributed to Cu $2p_{1/2}$. Peaks at 932.3 and 952.3 eV in the Cu 2*p* spectrum were consistent with $Cu_2S$ [12, 13], meaning that the surface of the CZTS film was covered by the secondary phase $Cu_2S$. As the surface of the film was sputtered, $Cu_2S$ was sputtered as well. As a result, the peaks at 932.9 eV (Cu $2p_{3/2}$) and 952.7 eV (Cu $2p_{1/2}$) of the sputtered film originated from the Cu in CZTS [14]. Although it has been reported that ternary compounds such as $Cu_2SnS_3$ and $Cu_3SnS_4$ may also exist on the surface of CZTS films [6], these

compounds were not identified in the Cu 2*p* spectra because of either the overlap of Cu 2*p* peaks with $Cu_2S$ or the absence of these phases.

Figure 3(b) displays the Zn 2*p* spectra obtained at different depths in the CZTS film. The peak alignment was similar to that of Cu 2*p* (Fig. 2(a)). At the film surface (before sputtering), the peak at 1021.9 eV with a full-width at half-maximum of 1.7 eV was consistent with Zn $2p_{3/2}$ of ZnS, and that at 1045.0 eV was attributed to Zn $2p_{1/2}$ of ZnS [15]. After the film was sputtered, both Zn $2p_{3/2}$ and $2p_{1/2}$ peaks increased in intensity and their positions remained at the same binding energies. This indicates that the chemical state of Zn was the same throughout the CZTS layer. As a result, the CZTS film had Zn binding energies of 1022.3 eV for $2p_{3/2}$ and 1045.4 eV for $2p_{1/2}$. After the film was sputtered to a depth of 1.4 μm, the intensity of the peaks was very weak, indicating that the bottom of the CZTS film had been reached.

The Sn 3*d* spectra obtained at different depths in the CZTS film are presented in Fig. 3(c). The sample before sputtering showed two peaks at 486.4 and 494.8 eV corresponding to Sn $3d_{5/2}$ and Sn $3d_{3/2}$, respectively [16]. The peak at 486.4 eV is consistent with Sn $3d_{5/2}$ in SnS, meaning the secondary phase SnS exists on the film surface [17]. After the film was sputtered to a depth of 40 nm (sputtering time: 1 min), the Sn $3d_{5/2}$ peak shifted to 486.8 eV, which is assigned to Sn $3d_{5/2}$ in $SnS_2$ [18], indicating that the dominant secondary phase is $SnS_2$ rather than SnS in the sub-surface region of the CZTS layer. When the CZTS film was sputtered to a depth of 80 nm (sputtering time: 2 min), this peak shifted to 486.6 eV and then remained fixed with further sputtering. Thus, this peak was attributed to Sn $3d_{5/2}$ in CZTS. The intensities of the peaks attributed to secondary phases containing Sn were comparable or stronger than those of the peaks of CZTS. This is caused by the easy formation of SnS compounds during annealing. When the film was sputtered to a depth of 1.4 μm (sputtering time: 35 min), almost no peaks were observed in the Sn 3*d* spectrum.

Figure 3(d) shows the S 2*p* spectra obtained at different depths in the CZTS film. The peak at a binding energy of around 161 eV was attributed to S $2p_{3/2}$, while that at around 163 eV originated from S $2p_{1/2}$. Although it was concluded that the secondary phases CuS, ZnS, and $SnS_x$ ($x$=1, 2) existed on the surface of the CZTS film judging from the Cu 2*p*, Zn 2*p*, and Sn 3*d* spectra, only two peaks at 161.7 and 162.9 eV were detected for the surface S 2*p* spectra of the CZTS film because of the similar binding energies of S in ZnS (around 162.7 eV), CuS (around 162.5 eV), and $SnS_x$ ($x$=1, 2) (161.1 eV) [18]. The inset in Fig. 3(d) displays a magnified spectrum of S near the interface between CZTS and Mo. Two peaks at 161.9 and 163.1 eV were identified. Formation of $MoS_2$ at CZTS–Mo interfaces has been widely

 doi:10.20944/preprints201701.0064.v1

reported [19-21]. The S 2*p* spectrum of $MoS_2$ contains two separate peaks at 161.9 and 163.1 eV [22]. As a result, one possible assignment for these peaks is S $2p_{3/2}$ of $MoS_2$ for the peak at 161.9 eV and S $2p_{1/2}$ of $MoS_2$ for that at 163.1 eV, although this requires further confirmation. The above spectra indicate that the surface of the CZTS film is covered by a thin layer (less than 40 nm thick) of secondary phases including CuS, ZnS, and SnS, followed by a thin layer (less than 40 nm thick) of the secondary phase $SnS_2$ between the top secondary-phase layer and the CZTS bulk.

The interface between CZTS and Mo was further studied to confirm the existence of $MoS_2$ by measuring the chemical state of Mo. Generally, the electrons in 3*d* orbitals display stronger XPS peak intensities than electrons in other orbitals for Mo species. Figure 4 shows the Mo 3*d* spectra obtained at different depths in the CZTS film. The standard Mo spectrum has two peaks located at binding energies of 227.7 eV for $3d_{5/2}$ and 230.9 eV for $3d_{3/2}$, which are marked in Fig. 4. When CZTS was sputtered to a depth of 600 nm (sputtering time: 15 min), only a small peak was detected. To make this peak clear, the spectrum of Mo around 227.7 eV was magnified, as shown in the inset of Fig. 4. The very weak Mo spectrum was attributed to the Mo film beneath the cracks in the CZTS film, which allowed source X-rays and photoelectrons from Mo to pass through. Although cracks also exist at the surface of CZTS, they are covered by a layer of secondary phases, which leads to Mo being almost undetected in the CZTS film. When the film was sputtered to a depth of 1.4 μm (sputtering time: 35 min), two strong peaks appeared at binding energies of 229.6 and 233.0 eV, both of which were assigned to Mo 3*d* [23]. By checking the XPS database, these peaks were attributed to Mo in $MoS_2$, which displays two peaks located at around 229 eV for $Mo_{5/2}$ and around 233 eV for $3d_{3/2}$ [18]. These results are consistent with those obtained above for S. Therefore, the presence of a $MoS_2$ layer between CZTS and Mo was confirmed by XPS analysis.

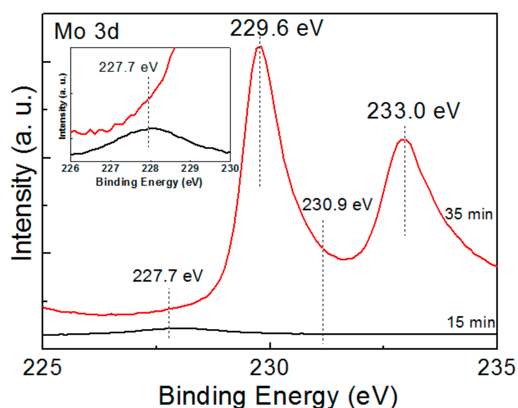

doi:10.20944/preprints201701.0064.v1

FIG. 4 Mo 3*d* spectrum at a depth of 600 nm (sputtering time: 15 min) and the interface between CZTS and the Mo substrate (sputtering time: 35 min). The peak positions of elemental Mo at 227.7 eV assigned to Mo $3d_{5/2}$ and 231.0 eV attributed to Mo $3d_{3/2}$ are marked in the spectra. The inset is a magnified view of the Mo spectrum around a binding energy of 227.7 eV.

## 4. Conclusion

In summary, the secondary phases in an annealed CZTS film were detected by XPS. After CZTS films were annealed in a S atmosphere, adsorbed molecular oxygen existed on the surface of the film. No oxygen was detected in the film bulk. The surface of the CZTS film was covered by a thin layer (less than 40 nm thick) of secondary phases including CuS, ZnS, and Sn. Below this layer, there was another secondary-phase thin layer (less than 40 nm thick) of $SnS_2$. The total thickness of the region with secondary phases was less than 80 nm. In addition, ternary phases such $Cu_2SnS_3$ were not identified because of the absence of characteristic peaks in Cu and Sn spectra and lack of information about these compounds in the XPS database. Formation of $MoS_2$ at the CZTS–Mo interface was confirmed by XPS analysis of S and Mo.

This work was partly supported by Waseda University Initiatives and a Waseda University Grant for Special Research Projects.

## References

[1]S. Chen, X. G. Gong, A. Walsh, and S.H. Wei, Appl. Phys. Lett. **94**, 041903 (2009).

[2]W. Ki, and H. W. Hillhouse, Adv. Energy Mater. **1**, 732 (2011).

[3]V. A. Akhavan, B. W. Goodfellow, M. G. Panthani, C. Steinhagen, T. B. Harvey, C. J. Stolle, and B. A. Korgel, J. Sol. State Chem. **189**, 2 (2012).

[4]W. Wang, M. T. Winkler, O. Gunawan, T. Gokmen, T. K. Todorov, Y. Zhu, D. B. Mitzi, Adv. Energy Mater. **4**, 1301465 (2013).

[5]I. D. Olekseyuk, I. V. Dudchak, and L. V. Piskach, J. Alloys Compd. **368**, 135 (2004).

[6]X. Fontané, L. Calvo-Barrio, V. Izquierdo-Roca, E. Saucedo, A. Pérez-Rodriguez, J. R. Morante, D. M. Berg, P. J. Dale and S. Siebentritt, Appl. Phys. Lett. **98**, 181905 (2011)

[7]A. Fairbrother, E. García-Hemme, V. Izquierdo-Roca, X. Fontané, F. A. Pulgarín-Agudelo, O. Vigil-Galán, A. Pérez-Rodríguez and E. Saucedo, J. Am. Chem. Soc. **134**, 8018 (2012).

[8]A. J. Cheng, M. Manno, A. Khare, C. Leighton, S. A. Campbell, and E. S. Aydi, J. Vac. Sci. Technol. A 29, 051203-1 (2011).

 doi:10.20944/preprints201701.0064.v1

[9]X.F. Zhang, Y. Umejima, and M. Kobayashi, Fabrication of $Cu_2ZnSnS_4$ (CZTS) Nanoparticle Inks by a Ball Milling Method for the Growth of CZTS Films. Submitted.

[10]J. J. Scragg, T. Ericson, T. Kubart, M. Edoff, and C. Platzer-Björkman, Chem. Mater. **23**, 4625 (2011).

[11]K. Prabhakaran, and C.N.R. Rao, Surf. Sci. **186**, L575-L580 (1987).

[12]T. Abe, Y. Kashiwaba, M. Baba, J. Imai, and H. Sasaki, Appl. Surf. Sci. **175-176**, 549 (2001).

[13]V. Krylova and M. Sndrulevičius, Int. J. Photoenergy. 304308, (2009).

[14]M. Aono, K. Yoshitake, and H. Miyazaki, Phys. Status. Solidi C **10**, 1058 (2013).

[15]D. Barreca, Surf. Sci. Spectra. **9**, 54 (2002).

[16]M. Salavati-Niasari, D. Ghanbari, and F. Davar, J. Alloys. Compd. **492**, 570 (2010).

[17]M. V. Reddy, P. Babu, K. T. R. Reddy and R. W. Miles, J. Renewable Sustainable Energy **5**, 031613 (2013).

[18]A. V. Naumkin, A. Kraut-Vass, S. W. Gaarenstroom, and C. J. Powell, NIST X-ray Photoelectron Spectroscopy Database, http://srdata.nist.gov/xps/.

[19]F. Liu, K. Sun, W. Li, C. Yan, H. Cui, L. Jiang, X. Hao and M. A. Green, Appl. Phys. Lett. **104**, 051105 (2014).

[20]K. J Yang, J. H. Sim, B. Jeon, D. H Son, D. H. Kim, S. J. Sung, D. K. Hwang, S. Song, D. B. Khadka, J. H. Kim, and J. K Kang, Prog. Photovolt: Res. Appl. **23**, 862 (2015).

[21]D. Seo, C. Kim, E. Oh, C. W. Hong, J. H. Kim, and S. Lim, J. Mater. Sci.: Mater. Electron. **25**, 3420 (2014).

[22]H. W. Wang, P. Skeldon, G. E. Thompson, Surf. Coat. Technol. **91**, 200 (1997).

[23]C. D. Wagner, W. M. Riggs, L. E. Davis, and J. F. Moulder. *HANDBOOK of X-RAY PHOTOELECTRON SPECTROSCOPY* (Perkin-Elmer Corporation, Minnesota, 1979) p. 104.

© 2017 by the authors; licensee *Preprints*, Basel, Switzerland. This article is an open access article distributed under the terms and conditions of the Creative Commons by Attribution (CC-BY) license (http://creativecommons.org/licenses/by/4.0/).